Journal of Colloid and Interface Science **217,** 219–236 (1999)
Article ID jcis.1999.6354, available online at http://www.idealibrary.com on IDEAL®

FEATURE ARTICLE

Electrical Interaction Energy between Two Charged Entities in an Electrolyte Solution

Jyh-Ping Hsu[1] and Bo-Tau Liu

Department of Chemical Engineering, National Taiwan University, Taipei, Taiwan 10617, Republic of China

Received April 5, 1999; accepted May 28, 1999

The electrical interaction energy between two charged entities in an electrolyte solution plays a significant role in various phenomena in colloid and interface science. Available methods for the estimation of this energy under the Debye–Huckel condition are discussed briefly, and a systematic approach based on a boundary integral method, which has the potential to yield an approximate analytical expression for various types of surfaces under a general surface condition, is introduced. The linear sizes of the interacting entities can be comparable or one is much larger than the other. A typical example for the former includes, for instance, the interaction between two colloidal particles. The stability behavior of a colloidal dispersion belongs to this category. That for the latter includes the interaction between a particle and a wall. The adsorption of particles to surfaces and the electrophoretic motion of particles near a boundary, for example, belong to this category. Extensions to more complicated cases, for example, multiple particles and arbitrary surfaces, are also discussed. © 1999 Academic Press

Key Words: **charged entities; electrical interaction energy; boundary integral method; Poisson–Boltzmann equation; Debye–Huckel condition.**

1. INTRODUCTION

Particulate and interfacial sciences and technologies are foundations to modern chemical process industrials including such diverse areas as fertilizers, foods, minerals, materials, and energy. Indeed, a majority of the value added by the modern industry is directly related to them. An across-the-board assessment also reveals that they will play the key role in high-tech industries, for example, electronics, advanced materials, biotechnology, and environment, to name a few, of the coming century. A detailed understanding of the mechanisms and phenomena involved is essential not only to the development of new technologies but also to fundamental studies. Often, evaluation of the electrical interaction energy between two charged entities needs to be estimated in the description of the relevant analyses. The broad spectrum of particulate science and interfacial sciences includes various possible combinations of solid, liquid, and gas phases. In the discussion below, we will focus only on the case in which solid entities are dispersed in a liquid phase containing electrolytes. Although the problem under consideration is classic and has been investigated extensively in the literature most of the discussions are limited to specific geometry or boundary conditions. A systematic approach has not been introduced.

On the basis of the relative magnitudes of the interacting entities, two types of problem can be identified: the sizes of the two interacting entities are comparable, and one of two interacting entities is orders of magnitude larger than the other. The coagulation phenomenon of a colloidal suspension in water and wastewater treatment, for example, belongs to the former. Here, the stability behavior of the dispersed system is of main concern. The classic analysis (DLVO theory) for an aqueous dispersion of lyophobic colloidal particles involves the calculation of the electrical and van der Waals interactions between two charged particles (1). The goal here is to seek conditions, which lead to an unstable system; that is, the attractive force between two particles overcomes the repulsive force between them, and coagulation between particles occurs. In some other cases, searching for conditions which yield a stable dispersion becomes the key issue. For instance, how to maintain the stability of the slurry used in chemical–mechanical polishing (2, 3) is essential to a wafer production process. The attachment of particles to surfaces is one of the typical examples in which the sizes of two interacting entities are orders of magnitude different. It is also possible that a problem involves both types of interactions. The electrophoretic motion of a particle in which either the effect of nearby particles or the presence of a boundary needs to be considered is one of the typical examples in practice.

Recent advances in direct force measurement techniques based on surface force apparatus (4, 5) allow an accurate estimation of the forces between charged particles and surfaces. Apparently, quantitatively identifying the electrical force is essential to the estimation of various other possible interac-

[1] To whom correspondence should be addressed.

0021-9797/99 $30.00

tion forces, e.g., hydration force, steric force, and van der Waals force, involved when two entities approach each other. The purpose of this work is to summarize briefly the available methods in the literature for the evaluation of the electrical interaction energy between two charged entities and to introduce a systematic approach based on a boundary integral method. The latter is capable of leading to an approximate analytical result for problems often encountered in practice. We will limit the discussion to a low to medium level of electrical potential mainly for two reasons. First, estimating the interaction energy analytically for an arbitrary level of electrical potential can be done only for extremely limited cases, and a numerical scheme is required for most of the problems. Second, if the electrical potential is high, there is a lack of rigorous governing equation for the description of its spatial variation. The discussion ends with a brief description of the problems that are of both practical and theoretical significance and deserve further study in the near future.

2. BASIC EQUATIONS

The estimation of the electrical interaction energy between two charged entities comprises two steps in a series: determine the spatial variation in the electrical potential, and conduct an integration over a specified domain which simulates a charging process.

2.1. Electrical Potential

At equilibrium, assuming that the distributions of electrolyte ions in the liquid phase follow the Boltzmann distribution, the spatial variation of electrical potential of the system under consideration can be described approximately by the so-called Poisson–Boltzmann equation. This equation needs to be solved subject to the boundary conditions reflecting the nature of the charged entities and the domain considered.

2.1.1. Poisson–Boltzmann Equation

Suppose that the electrolyte ions can be treated as point charges. Then the ionic flux of ion species i, N_i, comprises the contribution due to concentration gradient and that due to electrical field, called the Nernst–Planck relation:

$$N_i = -D_i\left(\nabla n_i + \frac{Z_iF}{RT}\, n_i \nabla\psi\right). \qquad [1]$$

Here ∇ denotes the gradient operator; F and R are, respectively, the Faraday constant and the gas constant; D_i, Z_i, and n_i, are, respectively, the diffusivity, the valence, and the concentration of ion species i; and ψ is the electrical potential. Applying the condition that ions are unable to penetrate the surface of a rigid entity, Eq. [1] leads to

$$n_i = n_{i\infty}\exp\left(-\frac{Z_iF\psi}{RT}\right), \qquad [2]$$

where $n_{i\infty}$ is the bulk value of n_i. That is, the spatial variation of ions follows the Boltzmann distribution. Suppose that the permittivity of the liquid phase, ϵ, is constant. Then the relationship between electrical potential and space charge density ρ is

$$\nabla^2\psi = -\frac{\rho}{\epsilon}, \qquad [3]$$

where ∇^2 denotes the Laplace operator. The space charge density can be expressed as

$$\rho = \sum_i n_iZ_iF, \qquad [4]$$

where the summation is over all the charged species in the liquid phase. Substituting Eqs. [2] and [4] into Eq. [3] gives

$$\nabla^2\psi = -\frac{F}{\epsilon}\sum_i Z_in_{i\infty}\exp\left(-\frac{Z_iF\psi}{RT}\right). \qquad [5]$$

This is the Poisson–Boltzmann equation. Although its statistical mechanical grounds have been questioned, the performance of Eq. [5] in describing the diffuse double layer near a charged surface in an electrolyte solution is found to be satisfactory (6).

For symmetric Z:Z electrolytes, Eq. [5] becomes

$$\nabla^2 y = \kappa^2\sinh y, \qquad [6]$$

where the scaled potential y is defined by $y = ZF\psi/RT$, and $\kappa^2 = 2F^2Z^2C/\epsilon RT$, κ being the reciprocal Debye length. Gouy and Chapman (1, 6) were able to derive an analytic solution of Eq. [6] for an infinite planar surface. For other geometries and unsymmetric electrolytes, solving Eq. [5] analytically becomes difficult. Hsu and Liu (7) were able to derive a perturbation solution for a spheroidal surface in a symmetric electrolyte solution, and Hsu and Kuo (8) obtained a semi-analytical result for cylinderical and spherical surfaces. If the electrical potential is sufficiently low, Eq. [5] can be approximated by

$$\nabla^2\psi = \kappa^2\psi, \qquad [7]$$

the so-called Debye–Huckel approximation. The linear nature of this expression makes it easier to be solved than Eq. [6]. Unfortunately, if more than one charged surface is present, exactly solvable cases are still very limited.

2.1.2. Boundary Conditions

Various types of surface conditions are possible in practice. We will consider three cases, which are assumed mostly in the relevant analyses.

2.1.2.1. Constant potential/charge surfaces. Suppose that the electrical potential on an entity surface remains constant, that is,

$$\psi = \psi_S, \tag{8}$$

where ψ_S denotes the surface potential, which can be position dependent. If the surface charges arise from a surface reaction, or the exchange of potential determining ions with the bulk liquid phase, then assuming a constant surface potential is equivalent to assuming that the rate of surface reaction or that of exchanging of potential determining ions occurs infinitely fast. Equation [8] is a Dirichlet-type condition.

If the charge density on the entity surface σ_i is fixed, we have

$$\sigma = \sigma_i. \tag{9}$$

Compared with the case of constant surface potential, this is equivalent to assuming that the rate of surface reaction or that of exchanging of potential determining ions occurs infinitely slow. Note that if the permittivity of the solid phase is much smaller that of the liquid phase, then applying the Gauss divergence theorem leads to, at entity surface, $\sigma = -\epsilon(\partial\psi/\partial n)$. Therefore, Eq. [9] can be viewed as a Neumann-type condition.

2.1.2.2. Charge-regulated surfaces. Under certain circumstances the surface of an entity is capable of regulating its charged condition as a response to the variation in the nearby environment. A typical example includes surfaces of an amphoteric nature such as biological surfaces (9–17). Let us consider the case where the following surface reactions occur:

$$AB_2^{Z+} \leftrightarrow AB + B^{Z+} \tag{10a}$$

$$AB \leftrightarrow A^{Z-} + B^{Z+}. \tag{10b}$$

In these expressions, AB denotes the functional group, and B^{Z+} is the potential determining ion, Z being its valence. For amphoteric surfaces, B^{Z+} is usually the hydrogen ion (6). Let K_+ and K_-, be the dissociation constants of Eqs. [10a] and [10b], respectively. The net surface charge density can be evaluated by (11)

$$\sigma = \sigma_0 \frac{\delta \sinh[(\psi_N - \psi_S)/\psi_0]}{1 + \delta \cosh[(\psi_N - \psi_S)/\psi_0]}, \tag{11}$$

where $\sigma_0 = eZN_S$, $\psi_0 = RT/F$, $\psi_N = 2.303(\mathrm{p}K_0 - \mathrm{p}B)\psi_0$, $\mathrm{p}K_0 = (\mathrm{p}K_+ + \mathrm{p}K_-)/2$, $\Delta\mathrm{p}K = \mathrm{p}K_- - \mathrm{p}K_+$, and $\delta = 2 \times 10^{-\Delta\mathrm{p}K/2}$. In these expressions, N_S and T are the number density of the functional group and the absolute temperature, respectively, ψ_N is the Nernst potential, which is related to the point of zero charge when $\mathrm{p}K_0 = \mathrm{p}B$. A surface with a low $\Delta\mathrm{p}K$ is capable of regulating its charged condition efficiently so that its surface potential is more or less constant as the separation distance between two surfaces varies (18). In contrast, a surface with a high $\Delta\mathrm{p}K$ is considered to have properties close to those with a constant surface charge.

Note that if ψ_S is low, Eq. [11] can be approximated by

$$\sigma = \sigma_0 \frac{\delta \sinh(\psi_N/\psi_0)}{1 + \delta \cosh(\psi_N/\psi_0)} - \frac{\delta \cos(\psi_N/\psi_0) + \delta^2}{[1 + \delta \cosh(\psi_N/\psi_0)]^2} \frac{\sigma_0}{\psi_0} \psi_S$$

$$= \Xi - \Gamma\psi_S \tag{12}$$

with

$$\Xi = \sigma_0 \frac{\delta \sinh(\psi_N/\psi_0)}{1 + \delta \cosh(\psi_N/\psi_0)} \tag{12a}$$

$$\Gamma = \frac{\delta \cosh(\psi_N/\psi_0) + \delta^2}{[1 + \delta \cosh(\psi_N/\psi_0)]^2} \frac{\sigma_0}{\psi_0}. \tag{12b}$$

Equation [12] indicates that the boundary condition is of mixed nature. Note that the constant surface potential and constant charge density conditions, represented by Eqs. [8] and [9], respectively, can be recovered as the special cases of Eq. [12].

2.1.2.3. Charged membranes. Another important class of charged entities is that which has a porous or ion-penetrable, charged surface layer. Typical example includes biological cells, e.g., blood cells and protein aggregates (19–24), and entities covered by an artificial membrane, e.g., particles with an adsorbed polymer layer and porous entities (25, 26). These particles are characterized by having its fixed charges distributed over a finite volume in space, rather than over a rigid surface. In this case, an additional source term needs to be added to the right-hand side of Eq. [5] for a point inside membrane to reflect the presence of fixed charges, i.e.,

$$\nabla^2\psi = -\frac{F}{\epsilon} \sum_i Z_i n_{i\infty} \exp\left(-\frac{Z_i F \psi}{RT}\right) - \frac{\rho_f}{\epsilon}, \tag{13}$$

where ρ_f denotes the density of fixed charges.

2.2. Electrical Interaction Energy

If the surfaces of two rigid entities remain at constant potential, the electrical interaction energy, V_{el}, can be evaluated by

$$V_{el} = -\int_S \int_0^{\psi_S} \Delta\sigma(\psi_S')d\psi_S' dS, \quad [14]$$

where $\Delta\sigma = \sigma - \sigma_{iso}$, σ and σ_{iso} being, respectively, the surface charge density of a particle when both particles are present and that of an isolated particle. If the surface potential is low, Eq. [14] becomes

$$V_{el} = -\frac{1}{2}\int_S \Delta\sigma\psi_S dS. \quad [14a]$$

If two particles remain at constant surface charge density, then

$$V_{el} = \int_S \int_0^{\sigma} \Delta\psi_S(\sigma')d\sigma' dS, \quad [15]$$

where $\Delta\psi_S = \psi_S - \psi_{iso}$, ψ_{iso} being the surface potential of an isolated particle. If ψ_S is low, Eq. [15] becomes

$$V_{el} = \frac{1}{2}\int_S \sigma\Delta\psi_S dS. \quad [15a]$$

For two charge-regulated hard spheres, Carnie and Chan (27) were able to derive the following expression:

$$V_{el} = \int_S \left[\int_0^{\sigma} \Delta\psi_S^d(\sigma')d\sigma' - \int_0^{\sigma} \Delta\psi_S^S(\sigma')d\sigma'\right] dS. \quad [16]$$

Here, $\Delta\psi_S^S = \psi_S^S - \psi_{iso}^S$, ψ_{iso}^S being the value of ψ_S^S for an isolated particle, is the relation between surface potential and surface charge density that has to be satisfied as a result of surface reactions such as Eq. [10], and the function $\Delta\psi_S^d = \psi_S^d - \psi_{iso}^d$, ψ_{iso}^d being the value of ψ_S^d for an isolated particle, the surface potential calculate according to the Poisson–Boltzmann equation. For low electrical potentials, Eq. [16] becomes, after applying Eqs. [7] and [12],

$$V_{el} = \frac{1}{2}\Xi\int_S \Delta\psi_S dS. \quad [17]$$

For an ion-penetrable membrane which is capable of regulating its charged conditions, an expression which is similar to the case of a hard sphere with a charge-regulated surface can be written

$$V_{el} = \int_V \left[\int_0^{\sigma_i} \Delta\psi_S^d(\sigma_i')d\sigma_i' - \int_0^{\sigma_i} \Delta\psi_S^S(\sigma_i')d\sigma_i'\right] dV, \quad [18]$$

where V is the volume of membrane phase. For low electrical potentials, Eq. [18] becomes, after applying Eqs. [7] and [12],

$$V_{el} = \frac{1}{2}\Xi\int_V \Delta\psi_S dV. \quad [19]$$

As presented in the Appendix, the electrical interaction energy can also be evaluated based on Maxwell stress and osmotic pressure (28).

3. SOLUTION METHODS

Evaluation of the electrical interaction energy between two charged entities is nontrivial, in general, even for simple geometry at low electrical potentials. An analytical expression can be obtained only for very limited cases. McCormack *et al.* (29), for example, derived the electrical double-layer force and interaction free energy between two planar surfaces of various surface conditions in a symmetric electrolyte solution. In practice the interaction energy is evaluated either by a direct numerical integration or by an approximate analytical method. The latter, although not exact, is capable of providing a simple expression, which is highly desirable for subsequent analysis. In statistical mechanics, the difficulty of estimating the electrical interaction energy between two charged entities is often circumvented either by assuming a primitive model (30–32) or by assuming that it has the Yukawa form (33). The latter is based on the assumption that the double layer near a charged surface is thick and/or the separation between two entities is large (34, 35). Other approaches include that proposed by Derjaguin and Landau (36) and linear superposition. The latter is appropriate if the distance between two charged entities is longer than the Debye length; if this is not the case, the former becomes appropriate. Several attempts have been made in the past two decades to improve the performance of Derjaguin approximation (37–41). However, since the entity–entity distance can be in the medium range, a more satisfactory procedure is desirable for practical considerations. To this end, a systematic approach, which is applicable to a general charged condition, was proposed recently (42). A brief discussion about the available methods is given below.

3.1. Numerical Methods

Numerical methods provide a powerful and direct way of obtaining the solution of a problem, which is difficult to solve analytically. It avoids complicated mathematical treatments, and the result obtained is usually accurate. The finite difference method, which discretizes the computational domain into a

finite number of intervals (43–45), for example, is a useful tool for problems defined over a simple domain. If a global coordinate is difficult to be defined, e.g., two arbitrarily oriented spheroids, the finite element method, which discretizes the computational domain into a finite number of elements, can be applied. Problems using this method include, for example, two identical spheres (46), a cylinder and a plane (47), a biomacromolecule (48), a short cylinder (49), and a sphere and a charged pore (50). Due the degree of precision specified, however, numerical methods may face the convergence problem, and developing an efficient algorithm is essential. Also, parametric study can be tedious, and in view of the possible mathematical treatments in the subsequent analyses, a numerical solution is not as attractive as an analytical expression.

3.2. Approximate Analytical Methods

Several methods, which lead to approximate analytical results, are introduced briefly.

3.2.1. Derjaguin and Modified Derjaguin Approximations

Derjaguin (51) suggested that if two spheres are sufficiently close to each other, the interaction energy between them can be estimated based on that of two planar parallel surfaces. This method is appropriate if the closest surface-to-surface distance between two entities is on the order of Debye length. One of the popular applications based on Derjaguin's approximation is that proposed by Hogg *et al.* (52) for two rigid spheres; the result obtained is found to be accurate for thin double layers. Several attempts were made to improve the performance of Derjaguin's approximation for thicker double layers. Often, the solution of a Poisson–Boltzmann equation is estimated either by expanding the electrical potential based on the result of Gouy and Chapman, i.e., the solution for two parallel, planar surfaces, or through an iterative procedure based on that. Although these methods lead to better results the improvement in the degree of accuracy is limited, and sometimes the procedure involved can be tedious. Derjaguin's approximation can be modified to improve its performance for a moderate level of electrical potential (53, 54). It was also incorporated with another method (55).

3.2.2. Multipole Expansion

This approach is based on the assumption that the solution to a Poisson–Boltzmann equation can be expanded in a series of harmonic functions R_n

$$\psi = \sum_n C_n R_n. \qquad [20]$$

The coefficient C_n is determined by the associated boundary conditions based on the orthogonal property of R_n (56–59). The electrical potential obtained is then used to evaluate the interaction energy. The approach is semi-analytic, and its performance depends largely on the choice of harmonic functions and the number of terms used. It should be pointed out that choosing R_n adequately can be nontrivial for irregular surfaces. Also, if a mixed boundary condition such as Eq. [12] is assumed, then the orthogonal property of R_n becomes invalid. In this case C_n needs to be evaluated through solving a large set of simultaneous algebraic equations (60).

3.2.3. Boundary Collocation Method

This method is similar to multipole expansion. It is assumed that the solution to Eq. [7] can be approximated by a linear combination of a finite number of harmonic functions, i.e., the upper limit of n in Eq. [20] is a finite number M. After substituting the assumed solution into Eq. [7], sufficiently many points on the domain boundary are chosen so that coefficient C_n, $n = 1, 2, \ldots, M$, can be determined. A set of linear algebraic equations needs to be solved. As in multipole expansion, choosing an appropriate set of harmonic functions can be nontrivial for irregular surfaces. Also, its performance is usually unsatisfactory if the level of surface potential is high. Another problem is the choice of M. Often, a considerable amount of computing time is necessary to reach a convergent solution.

3.2.4. Boundary Integral and Boundary Element Methods

The boundary integral method is based on the fact that the solution of Eq. [7] can be expressed as an integral of its Green function over the boundary of problem domain. In other words, the dimensionality of the original problem can be reduced by one through adopting this approach. The boundary conditions are incorporated automatically into the integral representation of the solution of Eq. [7]. For irregular surfaces evaluating directly the integral is difficult, and it is approximated by a system of algebraic equations obtained through discretizing the boundary, the so-called boundary element method. The boundary integral method has the merit that it has the potential of obtaining an analytical solution. This, however, is often nontrivial even for regular surfaces. The boundary element method, in contrast, has the merit that it is more readily applicable to irregular surfaces. However, the results obtained are numerical, and developing an efficient algorithm can be time consuming.

3.2.5. Reflection Method

Let us label the entities in a system as entities 1 and 2. If $\psi^{(0)}$ denotes the potential due to the presence of isolated entity 1, then it will not satisfy the condition on the surface of entity 2. This is compensated for by adding a correction term $\psi^{(1)}$ to $\psi^{(0)}$. But now the corrected potential may not satisfy the condition on the surface of entity 1. Therefore the potential is further corrected by adding a new term $\psi^{(2)}$. This procedure is repeated

until the resultant potential satisfies the specified surface conditions. The final solution takes the form

$$\psi = \psi^{(0)} + \psi^{(1)} + \psi^{(2)} + \cdots. \quad [21]$$

In principle, an analytic expression can be obtained. It, however, is usually complicated (58, 61–63), and the rate of convergence can be a problem.

3.2.6. Linear Superposition

Linear superposition assumes that the result of multiple charged entities can be approximated by a linear combination of the results for individual entities. For instance, if ψ_1 and ψ_2 are the solutions of Eq. [7] for isolated entities 1 and 2, respectively, then the solution of Eq. [7] when both entities are present is approximated by

$$\psi = \psi_1 + \psi_2. \quad [22]$$

Analyses which applied this approach include, for example, two plates covered with charge-regulated layers (64), two spheres covered by an ion-penetrable membrane (16), and two spheroids (65). Although it is simple and straightforward, linear superposition is limited to the case when the distance between two entities is longer than two Debye lengths. Another possible case in which linear superposition is applicable is ion-penetrable entities. An image-interaction correction strategy was proposed by Ohshima (66) to improve the performance of linear superposition for the case of two dissimilar spheres. Similar to the case of the reflection method, however, the result obtained is complicated.

4. A SYSTEMATIC APPROACH BASED ON BOUNDARY INTEGRAL

In a recent study, Hsu and Liu (42) applied the boundary integral method to various types of entity–entity interactions. An approximate analytical expression for the electrical interaction energy between two charged entities can be derived through a systematic approach. Their approach is introduced in the following discussion. Let us consider two charged entities with boundaries S_1 and S_2, respectively, in an electrolyte solution. It can be shown by direct substitution that a particular solution to Eq. [7] is

$$G(\mathbf{r}) = \frac{\exp(-\kappa \mathbf{r})}{4\pi \mathbf{r}}, \quad [23]$$

where $\mathbf{r}$ is the scaled position vector from a fixed point charge, and G is the free Green function (67). Applying Green's first identity, the solution to Eq. [7] can be expressed as

$$\psi = \sum_{i=1}^{2} \int_{S_i} \left[\frac{G}{\epsilon} \sigma_i + \psi_{Si} \chi_i \right] dS, \quad [24]$$

where

$$\chi_i = \frac{\partial G}{\partial n_i}, \quad i = 1, 2. \quad [24a]$$

In these expressions, n_i is the normal vector of S_i toward the liquid phase, and ψ_{Si} and σ_i are, respectively, the surface potential and the surface charge density of entity i. The dielectric constant of the entities is assumed to be much smaller than that of the liquid phase. It can be shown that, for a point on S_j, we have (68)

$$\frac{1}{2} \psi_{Sj} = \sum_{i=1}^{2} \int_{S_i} \left[\frac{G}{\epsilon} \sigma_i + \psi_{Si} \chi_i \right] dS_i. \quad [25]$$

Consider the general linear boundary condition represented by Eq. [12],

$$\sigma_i = \Xi_i - \Gamma_i \psi_{Si}, \quad [26]$$

where Ξ_i and Γ_i are constant. If both Ξ_i and Γ_i are large, Eq. [26] yields a constant potential condition with $\psi_{Si} = \Xi_i/\Gamma_i$. If $\Gamma_i \to 0$, then the surface charge of S_i remains constant at $\sigma_i = \Xi_i$. Other than these cases, S_i can be regarded as a charge-regulated surface (10, 11, 14).

Substituting Eq. [26] into Eq. [25], we obtain

$$\frac{1}{2} \psi_{Sj} = \sum_{i=1}^{2} \int_{Si} \left\{ \frac{\Xi_i}{\epsilon} G + \left(\frac{-\Gamma_i}{\epsilon} G + \chi_i \right) \psi_{Si} \right\} dS_i. \quad [27]$$

Suppose that ψ_{Si} can be decomposed as

$$\psi_{Si} = \psi_{Si}^0 + \Delta \psi_{Si}, \quad [28]$$

where ψ_{Si}^0 is the unperturbed surface potential of isolated entity i, and $\Delta \psi_{Si}$ is a perturbed surface potential of entity i due to the presence of the other entity. Suppose that ψ_{Si}^0 is position-independent. Then

$$\psi_{Si}^0 = \frac{\dfrac{\Xi_i}{\epsilon} \beta_{ii}}{\dfrac{1}{2} + \dfrac{\Gamma_i}{\epsilon} \beta_{ii} - \gamma_{ii}}, \quad [29]$$

where

$$\beta_{ii} = \int_{Si} G_{ii} dS_i \qquad [29a]$$

$$\gamma_{ii} = \int_{Si} \chi_{ii} dS_i \qquad [29b]$$

In these expressions G_{ii} and χ_{ii} are, respectively, the values of G and χ_i when both of the two end points of the position vector are on S_i. Suppose that the electrical potential for isolated entity i can be expressed as

$$\psi_i = \psi^0_{Si}\theta_i, \qquad [30]$$

where θ_i is a function of the position in the liquid phase. Substituting Eqs. [28]–[30] into Eq. [27], we obtain

$$\frac{1}{2}\Delta\psi_{S1} = \int_{S_1}\left(\frac{-\Gamma_1}{\epsilon}G + \chi_1\right)\Delta\psi_{S1}dS_1 + \int_{S_2}\left(\frac{-\Gamma_2}{\epsilon}G + \chi_2\right)\Delta\psi_{S2}dS_2 + \psi^0_{S2}\theta_{12} \qquad [31a]$$

$$\frac{1}{2}\Delta\psi_{S2} = \int_{S_1}\left(\frac{-\Gamma_1}{\epsilon}G + \chi_1\right)\Delta\psi_{S1}dS_1 + \int_{S_2}\left(\frac{-\Gamma_2}{\epsilon}G + \chi_2\right)\Delta\psi_{S2}dS_2 + \psi^0_{S1}\theta_{21}, \qquad [31b]$$

where θ_{ji} is the value of θ_i when one of the end points of the position vector is on S_j. Equations [31a] and [31b] are implicit expressions for $\Delta\psi_{Sj}$, which have the form of an integral equation with an inseparable kernel, and, therefore, solving them directly is difficult. This difficulty can be circumvented by replacing approximately Eqs. [31a] and [31b] by a set of algebraic equations, which are readily solvable. The procedure is based on the fact that the surface integral of a smooth function Z can be approximated by

$$\int ZdS \cong \sum_{i=1}^{M} w_i Z_i, \qquad [32]$$

where w_i is a weighting factor, and Z_i is the value of Z at point i. The values of w_i and M depend on the integration scheme adopted. On the basis of Eq. [32] Eqs. [31a] and [31b] can be expressed as

$$\underline{\chi}\underline{\Delta\psi} = \underline{B}, \qquad [33]$$

where

$$\Delta\underline{\psi} = [\Delta\psi_{1,1}, \Delta\psi_{1,2}, \ldots \Delta\psi_{1,M}, \Delta\psi_{2,1}, \ldots, \Delta\psi_{2,M}]^t \qquad [33a]$$

$$\underline{\aleph} = \begin{bmatrix} \underline{\aleph}_{1,1} & \underline{\aleph}_{1,2} \\ \underline{\aleph}_{2,1} & \underline{\aleph}_{2,2} \end{bmatrix} \qquad [33b]$$

$$\underline{\aleph}_{l,k} = [\aleph_{i,j,l,k}], \quad i, j = 1, \ldots, M, \quad l, k = 1, 2 \qquad [33c]$$

$$\aleph_{i,j,l,k} = -w_j\left(\frac{-\Gamma_k}{\epsilon}G^{l,i}_{k,j} + \chi^{l,i}_{k,j}\right), \quad i, j = 1, \ldots, M, \quad l, k = 1, 2, \quad i \neq j \text{ or } l \neq k$$

$$= \frac{1}{2} - w_j\left(\frac{-\Gamma_k}{\epsilon}G^{l,i}_{k,j} + \chi^{l,i}_{k,j}\right), \quad i = j \text{ and } l = k, \quad i, j = 1, \ldots, M, \quad l, k = 1, 2 \qquad [33d]$$

$$\underline{B} = \begin{bmatrix} \psi^0_{S2}\theta_{12,1} \\ \cdot \\ \cdot \\ \psi^0_{S2}\theta_{12,M} \\ \psi^0_{S1}\theta_{21,1} \\ \cdot \\ \cdot \\ \psi^0_{S1}\theta_{21,M} \end{bmatrix}. \qquad [33e]$$

In these expressions, superscript t represents matrix transpose, $G^{l,i}_{k,j}$ and $\chi^{l,i}_{k,j}$ are, respectively, the values of G and χ in which the distance r is measured from point j of entity k to point i of entity l, and the differentiation is conducted on S_k, $\theta_{ji,k}$ denotes the values of θ_{ji} evaluated at point k of entity j. If $l = k$ and $i = j$, then $G^{l,i}_{k,j}$ and $\chi^{l,i}_{k,j}$ become singular. In this case the following approach is applicable. Equations [29a] and [29b] suggest that $G^{k,j}_{k,j}$ and $\chi^{k,j}_{k,j}$ can be evaluated by subtracting the contribution of all other $G^{l,i}_{k,j}$ and $\chi^{l,i}_{k,j}$ from G_{kk} and γ_{kk}, respectively, that is,

$$\aleph_{j,j,k,k} = \frac{1}{2} - \left(\frac{-\Gamma_k}{\epsilon}\beta_{kk} + \gamma_{kk}\right) + \sum_{\substack{i=1 \\ i\neq j}}^{M} w_i\left(\frac{-\Gamma_k}{\epsilon}G^{k,j}_{k,i} + \chi^{k,j}_{k,i}\right). \qquad [34]$$

For the present linear system the electrical interaction energy between two entities can be calculated by employing Eq. [17]

$$V_{el} = \frac{1}{2}\,\Xi_1 \int_{S_1} \Delta\psi_{S1} dS + \frac{1}{2}\,\Xi_2 \int_{S_2} \Delta\psi_{S2} dS. \qquad [35]$$

Since $\Delta\psi_{Si}$ usually varies smoothly over S_i, the dimensions of the matrices in Eq. [33] need not be large, and it can be solved efficiently. Substituting the solution of Eq. [33] into Eq. [35], the electrical interaction energy between two entities can be calculated.

4.1. Approximate Analytical Expression

Obtaining an approximate analytic form for $\Delta\psi_{Sj}$ is also possible by adopting the method proposed by McCartney *et al.* (69) and Bell *et al.* (28). According to Eqs. [23] and [24a], both G and χ_i become very large when a singular point is approached. This suggests that $\Delta\psi_{Si}$ on the right-hand sides of Eqs. [31a] and [31b] can be moved out from the integral sign, and we have

$$\left(\frac{1}{2} - \gamma_{11} + \frac{\Gamma_1}{\epsilon}\,\beta_{11}\right)\Delta\psi_{S1} + \left(\frac{\Gamma_2}{\epsilon}\,\beta_{12} - \gamma_{12}\right)\Delta\psi_{S2} = \psi^0_{S2}\theta_{12} \qquad [36a]$$

$$\left(\frac{\Gamma_1}{\epsilon}\,\beta_{21} - \gamma_{21}\right)\Delta\psi_{S1} + \left(\frac{1}{2} - \gamma_{22} + \frac{\Gamma_2}{\epsilon}\,\beta_{22}\right)\Delta\psi_{S2} = \psi^0_{S1}\theta_{21}, \qquad [36b]$$

where

$$\beta_{ji} = \int_{Si} G_{ji} dS \qquad [36c]$$

$$\gamma_{ji} = \int_{Si} \chi_{ji} dS. \qquad [36d]$$

Here G_{ji} and χ_{ji} are respectively the values of G and χ_i when one of the end points of the position vector is on S_i and the other on S_j, $j \neq i$. The relationship among β_{ii}, β_{ji}, γ_{ii}, and γ_{ji} will be discussed later. For the time being, we claim that

$$\beta_{ji} = \beta_{ii}\theta_{ji} \qquad [37a]$$

$$\gamma_{ji} = \left(\frac{1}{2} + \gamma_{ii}\right)\theta_{ji}. \qquad [37b]$$

It should be pointed out that Eq. [37b] is applicable only if the condition that, if σ_i is uniform, then the corresponding ψ^0_{Si} is also uniform, is satisfied. Equation [37a], however, does not have this limitation.

Solving Eqs. [36a] and [36b] for $\Delta\psi_{Sj}$, $j = 1, 2$, and substituting the resultant expressions into Eq. [35], we obtain

$$V^1_{el} = \frac{\epsilon}{2\beta_{11}} \int_{S_1} \frac{\psi^0_{S1}\psi^0_{S2} + f_2\psi^{0\,2}_{S1}\theta_{21}}{1 - f_1 f_2 \theta_{12}\theta_{21}}\,\theta_{12} dS \qquad [38a]$$

$$V^2_{el} = \frac{\epsilon}{2\beta_{22}} \int_{S_2} \frac{\psi^0_{S1}\psi^0_{S2} + f_1\psi^{0\,2}_{S2}\theta_{12}}{1 - f_1 f_2 \theta_{12}\theta_{21}}\,\theta_{21} dS, \qquad [38b]$$

where

$$f_1 = \frac{\dfrac{1}{2} + \gamma_{11} - \dfrac{\Gamma_{11}}{\epsilon}\,\beta_{11}}{\dfrac{1}{2} - \gamma_{11} + \dfrac{\Gamma_{11}}{\epsilon}\,\beta_{11}} \qquad [38c]$$

$$f_2 = \frac{\dfrac{1}{2} + \gamma_{22} - \dfrac{\Gamma_{22}}{\epsilon}\,\beta_{22}}{\dfrac{1}{2} - \gamma_{22} + \dfrac{\Gamma_{22}}{\epsilon}\,\beta_{22}}. \qquad [38d]$$

Employing the approximate procedure adopted by Sader *et al.* (53), Eqs. [38a] and [38b] can be rewritten, respectively, as

$$V^1_{el} = \frac{\epsilon}{2\beta_{11}} \int_{S_1} \left[\frac{\psi^0_{S1}\psi^0_{S2} + f_2\psi^{0\,2}_{S1}\theta_{12}}{1 - f_1 f_2 \theta^2_{12}}\right]\theta_{12} dS \qquad [39a]$$

and

$$V^2_{el} = \frac{\epsilon}{2\beta_{22}} \int_{S_2} \left[\frac{\psi^0_{S1}\psi^0_{S2} + f_1\psi^{0\,2}_{S2}\theta_{21}}{1 - f_1 f_2 \theta^2_{21}}\right]\theta_{21} dS. \qquad [39b]$$

4.2. Some Useful Relations

Referring to Fig. 1a, S_i is a simple closed surface, its interior and exterior are denoted by Ω^i and Ω^0, respectively. Let r be the distance between two points. r_{ii} represents the value of r when both of these points are on S_i, and r_{ri} represents the value of r when one of the two points is on S_i and the other point not on S_i. Referring to Fig. 1a, r^i_{ri} is the value of r_{ri} when one of its two points is on S_i and the other point in Ω^i, and r^0_{ri} is that of r_{ri} when one of its two points is on S_i and the other point in Ω^0. Also, G_{ii} and G_{ri} become the values of $G(r)$ when r is replaced by r_{ii} and r_{ri}, respectively, and β_{ji} and γ_{ji} needed to be replaced by β_{ri} and γ_{ri}, respectively. Since directly evaluating β_{ii}, β_{ri}, γ_{ii}, and γ_{ri} can be nontrivial we suggest using the procedure below.

Step 1. Determine β_{ii} and β_{ri}. Let S_1 be an infinitely thin charged shell with a uniform surface charge density σ_1. The

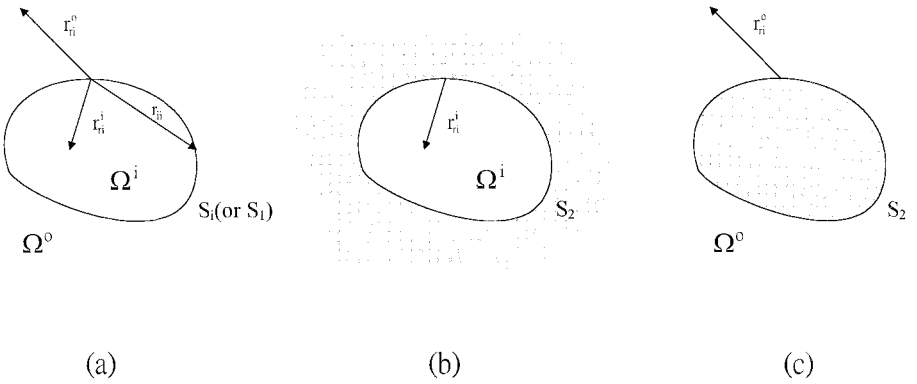

FIG. 1. (a) A simple closed surface S_1, with its interior Ω^i and exterior Ω^0. r is the distance between two points, r_{ii} represents the value of r when both of these points are on S_i, r_{ri}^i is the value of r when one point is on S_i and the other in Ω^i, and r_n^0 denotes that of r when one point is on S_i and the other in Ω^0. (b) A charged, simple closed surface S_2 with its interior Ω^i. (c) A charged, simple closed surface S_2 with its exterior Ω^0.

electrical potential inside the shell, ψ^i, and that outside the shell, ψ^0, can be expressed as

$$\psi^i = \psi_{S1}\theta^i \qquad [40a]$$

$$\psi^0 = \psi_{S1}\theta^0, \qquad [40b]$$

where ψ_{S1} is the surface potential, θ^i is a function of the position in Ω^i, and θ^0 is a function of the position in Ω^0. According to the Green's function theory (67), the spatial variation of electrical potential and the surface potential can be expressed, respectively, as

$$\psi = \frac{\sigma_1}{\epsilon}\beta_{ri} \qquad [41]$$

and

$$\psi_{S1} = \frac{\sigma_1}{\epsilon}\beta_{ii} \qquad [42]$$

Therefore,

$$\beta_{ii} = \frac{\epsilon\psi_{S1}}{\sigma_1}. \qquad [43]$$

If ψ_{S1} and σ_1 are known, then β_{ii} can be determined. It should be emphasized that Eq. [41] is valid if the distribution of surface charge is uniform. Equations [40a], [40b], [41], and [43] lead to

$$\beta_{ri}^i = \beta_{ii}\theta^i \qquad [44a]$$

$$\beta_{ri}^0 = \beta_{ii}\theta^0, \qquad [44b]$$

where β_{ri}^i and β_{ri}^0 are the values of β_{ri} associated with r_{ri}^i and r_{ri}^0, respectively.

Step 2. Determine γ_{ii} and γ_{ri}. To determine γ_{ii} and γ_{ri}, we consider the two cases shown in Figs. 1b and 1c. The former represents a charged, rigid surface S_2 with its interior, and the latter a charged, rigid surface S_2 with its exterior. The surface potential on S_2 is denoted as ψ_{S2}. It can be shown that the electrical potential inside S_2 for the case of Fig. 1b, ψ^i, and that outside S_2 for the case of Fig. 1c, ψ^0, can be expressed, respectively, as

$$\psi^i = \psi_{S2}\theta^i \qquad [45a]$$

and

$$\psi^0 = \psi_{S2}\theta^0. \qquad [45b]$$

Suppose that both the surface potential ψ_{S2} and the corresponding surface charge density σ_2 are position-independent. Then, according to Green's function theory, ψ^i and ψ^0 can also be expressed as

$$\psi^i = \frac{\sigma_2}{\epsilon}\beta_{ri}^i + \psi_{S2}\gamma_{ri}^i \qquad [46a]$$

$$\psi^0 = \frac{\sigma_2}{\epsilon}\beta_{ri}^0 + \psi_{S2}\gamma_{ri}^0 \qquad [46b]$$

and

$$\frac{1}{2}\psi_{S2} = \frac{\sigma_2}{\epsilon}\beta_{ii} + \psi_{S2}\gamma_{ii}. \qquad [46c]$$

TABLE 1
Results for β_{ii}, γ_{ii}, and θ_{ji} for Some Typical Geometries (42)

	β_{ii}	γ_{ii}	θ_{ji}
Rigid planar surface	$\frac{1}{2\kappa}$	0	$e^{-\kappa r}$
Outside a sphere	$\frac{1 - e^{-2\kappa a}}{2\kappa}$	$-\frac{1}{2}\left[\frac{1}{\kappa a} - \left(1 + \frac{1}{\kappa a}\right)e^{-2\kappa a}\right]$	$\frac{a}{r}e^{-\kappa(r-a)}$
Inside a sphere	$\frac{1 - e^{-2\kappa a}}{2\kappa}$	$\frac{1}{2}\left[\frac{1}{\kappa a} - \left(1 + \frac{1}{\kappa a}\right)e^{-2\kappa a}\right]$	$\frac{a}{r}\frac{\sinh(\kappa r)}{\sinh(\kappa a)}$
Outside a cylinder	$\frac{1}{\kappa\left[\frac{K_1(\kappa a)}{K_0(\kappa a)} + \frac{I_1(\kappa a)}{I_0(\kappa a)}\right]}$	$\frac{1}{\kappa\left[\frac{K_1(\kappa a)}{K_0(\kappa a)} + \frac{I_1(\kappa a)}{I_0(\kappa a)}\right]}$	$\frac{K_0(\kappa r)}{K_0(\kappa a)}$
Inside a cylinder	$\frac{1}{\kappa\left[\frac{K_1(\kappa a)}{K_0(\kappa a)} + \frac{I_1(\kappa a)}{I_0(\kappa a)}\right]}$	$\frac{1}{2} - \frac{\frac{I_1(\kappa a)}{I_0(\kappa a)}}{\left[\frac{K_1(\kappa a)}{K_0(\kappa a)} + \frac{I_1(\kappa a)}{I_0(\kappa a)}\right]}$	$\frac{I_0(\kappa r)}{I_0(\kappa a)}$

Note. r is the distance from a rigid planar surface, that from the center line of a cylindrical surface or that from the center of a spherical surface. a denotes the radius of a sphere or a cylinder. I_n and K_n are, respectively, the modified Bessel function of the first and the second kind of order n, $n = 0, 1$.

Therefore we have

$$\gamma_{ii} = \frac{1}{2} - \frac{\sigma_2}{\epsilon\psi_{S2}}\beta_{ii}. \quad [47]$$

Equations [45a]–[47] yield

$$\gamma_{ri}^{i} = \left(\frac{1}{2} + \gamma_{ii}\right)\theta^{i} \quad [48a]$$

$$\gamma_{ri}^{0} = \left(\frac{1}{2} + \gamma_{ii}\right)\theta^{0}, \quad [48b]$$

where γ_{ri}^{i} and γ_{ri}^{0} are the values of γ_{ri} associated with r_{ri}^{i} and r_{ri}^{0}, respectively. Note that, with θ^{i} and θ^{0} defined in steps 1 and 2, even if $S_1 = S_2$ and $\psi_{S1} = \psi_{S2}$, $\sigma_1 \neq \sigma_2$, in general. Table 1 summarizes the results for β_{ii}, γ_{ii}, and θ_{ji} for some typical cases (42).

4.3. Examples

Several examples are illustrated to justify the applicability of Table 1.

4.3.1. Two Spheres

Referring to Fig. 2, we consider two spherical particles in an electrolyte solution. These particles may have different sizes. R is the center-to-center distance between two particles, r_{21} is the distance between the center of particle 1 and the surface of particle 2, and a_1 and a_2 are the radii of particles 1 and 2, respectively. Applying Table 1, Eqs. [39a] and [39b] can be approximated, respectively, by

$$V_{\text{el}}^{1} = \frac{\pi\epsilon a_1 a_2}{\beta_{11}R}\int_{R-a_2}^{R+a_2}\frac{\psi_{S1}^{0}\psi_{S2}^{0} + f_2\psi_{S1}^{0}{}^{2}e^{-\kappa(r_{12}-a_2)}}{1 - f_1 f_2 e^{-2\kappa(r_{12}-a_2)}} \times e^{-\kappa(r_{12}-a_2)}dr_{12} \quad [49a]$$

and

$$V_{\text{el}}^{2} = \frac{\pi\epsilon a_1 a_2}{\beta_{22}R}\int_{R-a_1}^{R+a_1}\frac{\psi_{S1}^{0}\psi_{S2}^{0} + f_1\psi_{S2}^{0}{}^{2}e^{-\kappa(r_{21}-a_1)}}{1 - f_1 f_2 e^{-2\kappa(r_{21}-a_1)}} e^{-\kappa(r_{21}-a_1)}dr_{21}. \quad [49b]$$

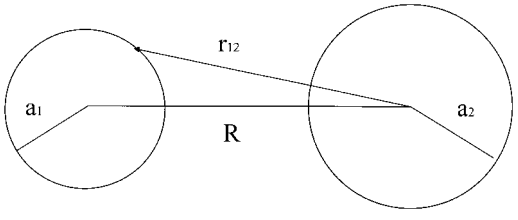

FIG. 2. Schematic representation of the system under consideration. R is the center-to-center distance between particles 1 and 2, r_{12} is the scaled distance between the center of particle 2 to a point on the surface of particle 1, and a_1 and a_2 are respectively the scaled radii of particles 1 and 2.

In the derivation of these expressions, θ_{ji} in the bracket of the right-hand side of Eqs. [39a] and [39b] is approximated respectively by $\exp[-\kappa(r_{12} - a_2)]$ and $\exp[-\kappa(r_{21} - a_1)]$, as was done in Sader *et al.* (53). For thin double layers, the following relations are applicable:

$$\ln(1 + ab) \cong b \cdot \ln(1 + a), \quad a, b \to 0, \qquad [50a]$$

$$\tan^{-1}(ab) \cong b \cdot \tan^{-1}(a), \quad a, b \to 0. \qquad [50b]$$

Summing Eqs. [49a] and [50b], and applying these relations, we obtain

$$V_{el} = \frac{\pi\epsilon a_1 a_2}{R}\left\{\frac{f_2\psi_{S1}^{0\,2} + f_1\psi_{S2}^{0\,2}}{f_1 f_2}\ln(1 - f_1 f_2 e^{-2\kappa(R-a_1-a_2)}) + \frac{4\psi_{S1}^0\psi_{S2}^0}{\sqrt{|f_1 f_2|}}\begin{bmatrix}\tan^{-1}(\sqrt{|f_1 f_2|}e^{-\kappa(R-a_1-a_2)}), & f_1 f_2 < 0\\ \tanh^{-1}(\sqrt{f_1 f_2}e^{-\kappa(R-a_1-a_2)}), & f_1 f_2 > 0\end{bmatrix}\right\}. \qquad [51]$$

The performance of this expression was found to be satisfactory, and the higher the ionic strength, the better the performance (42). For a constant surface potential ψ_{Si}, Eq. [51] becomes

$$V_{\rm el} = \epsilon\pi\frac{a_1 a_2}{R}\{(\psi_{S1} + \psi_{S2})^2\ln(1 + e^{-\kappa(R-a_1-a_2)}) + (\psi_{S1} - \psi_{S2})^2\ln(1 - e^{-\kappa(R-a_1-a_2)})\}. \qquad [52]$$

This is the same as that obtained by Sader *et al.* (53). For thin double layers, Eq. [51] can further be simplified as

$$V_{\rm el} = 4\pi\epsilon a_1 a_2\psi_{S1}^0\psi_{S2}^0\frac{e^{-\kappa(R-a_1-a_2)}}{R}. \qquad [53]$$

This expression can also be derived by neglecting the second term on the left-hand side of Eq. [36a] and the first term on the left-hand side of Eq. [36b] and substituting the resultant expressions into Eq. [35].

4.3.2. A Sphere and a Plane

As illustrated in Fig. 3, we consider a spherical particle (entity 2) of radius a_2 and a planar surface (entity 1). Let h be the closest surface-to-surface distance between them, let r_{21} be the distance between the planar surface and particle surface, and let r_{12} be the distance between the center of the particle and the planar surface. Applying Table 1, Eqs. [39a] and [39b] can be approximated, respectively, by

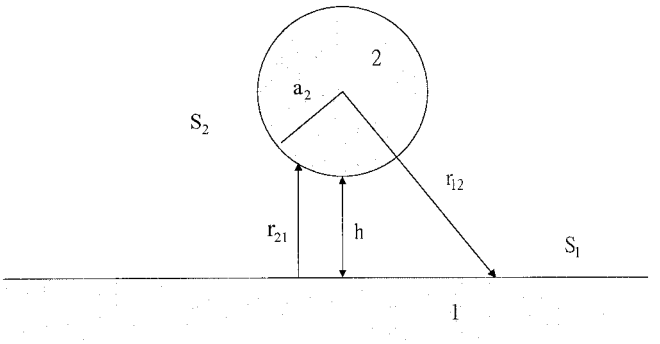

FIG. 3. A spherical particle (entity 2) of radius a_2 and a planar surface (entity 1). h is the closest surface-to-surface distance between particle and planar surface, r_{21} the distance from the planar surface to particle surface, and r_{12} the distance from the center of the particle to the planar surface.

$$V_{\rm el}^1 = \frac{\pi\epsilon a_2}{\beta_{11}}\int_{n+a_2}^{0}\frac{\psi_{S1}^{02} + f_2\psi_{S1}^{0\,2}e^{-\kappa(r_{12}-a_2)}}{1 - f_1 f_2 e^{-2\kappa(r_{12}-a_2)}}e^{-\kappa(r_{12}-a_2)}dr_{12} \qquad [54a]$$

$$V_{\rm el}^2 = \frac{\pi\epsilon a_2}{\beta_{22}}\int_{h}^{h+2a_2}\frac{\psi_{S1}^{02} + f_1\psi_{S2}^{0\,2}e^{-\kappa r_{21}}}{1 - f_1 f_2 e^{-2\kappa r_{21}}}e^{-\kappa r_{21}}dr_{21}. \qquad [54b]$$

In the derivation of Eq. [54a], θ_{21} in the bracket of the right-hand side of Eq. [39a] is approximated by $\exp[-\kappa(r_{12} - a_2)]$, as was done in Sader *et al.* (53). For thin double layers, summing Eq. [54a] and [54b], and applying Eqs. [50a] and [50b], we obtain

$$V_{\rm el} = \pi\epsilon a_2\left\{\frac{f_2\psi_{S1}^{0\,2} + f_1\psi_{S2}^{0\,2}}{f_1 f_2}\ln(1 - f_1 f_2 e^{-2\kappa h}) + \frac{4\psi_{S1}^0\psi_{S2}^0}{\sqrt{|f_1 f_2|}}\begin{bmatrix}\tan^{-1}(\sqrt{|f_1 f_2|}e^{-\kappa h}), & f_1 f_2 < 0\\ \tanh^{-1}(\sqrt{f_1 f_2}e^{-\kappa h}), & f_1 f_2 > 0\end{bmatrix}\right\}. \qquad [55]$$

This expression is similar to that derived by Carnie and Chan (27), which was based on Deryaguin's approximation. It was shown that, regardless of the types of surface condition, the performance of Eq. [55] is satisfactory and is better than that based on Deryaguin's approximation (42).

4.3.3. Sphere in a Planar Slit

Referring to Fig. 4, we consider a spherical particle (entity 2) of radius a_2 in a planar slit S_1 (entity 1) of width L. The latter comprises two surfaces, S_1^a and S_1^b. Let h_1 and h_2 be, respectively, the closest surface-to-surface distance between particle and S_1^a and that between particle and S_1^b, r_{21} be the distance from S_1 to particle surface, S_2, and r_{12} be the distance from the center of the particle to S_1. For the present case, since S_1 is the union of S_1^a and S_1^b, we have

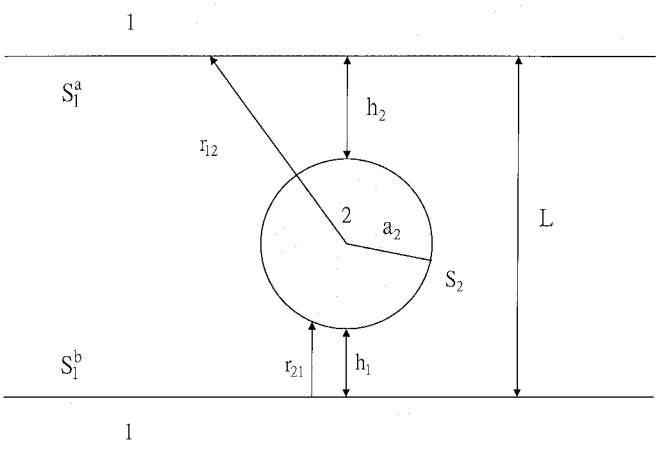

FIG. 4. A spherical particle (entity 2) of radius a_2 in a planar slit S_1 (entity 1) of width L, $S_1 = S_1^a \cup S_1^b$. h_1 and h_2 are, respectively, the closest surface-to-surface distance between particle and S_1^a and between particle and S_1^b, r_{21} is the distance from S_1 to particle surface, S_2, and r_{12} the distance from the center of particle to S_1.

$$\beta_{11} = \beta_{aa}^1 + \beta_{ab}^1 = \frac{1}{2\kappa} + \frac{e^{-\kappa L}}{2\kappa} = \frac{1 + e^{-\kappa L}}{2\kappa} \qquad [56a]$$

$$\gamma_{11} = \gamma_{aa}^1 + \gamma_{ab}^1 = 0 + \frac{e^{-\kappa L}}{2} = \frac{e^{-\kappa L}}{2}. \qquad [56b]$$

It can be shown that for two planar, parallel surfaces with a surface-to-surface distance L,

$$\theta_{ji} = \frac{e^{-\kappa r} + e^{-\kappa(L-r)}}{1 + e^{-\kappa L}}. \qquad [57]$$

On the basis of Eqs. [56a], [56b], [57] and Table 1, Eqs. [39a] and [39b] can be approximated, respectively, by

$$V_{\mathrm{el}}^1 = \frac{\epsilon a_2}{2\beta_{11}} \int_{S_1} \frac{\psi_{S1}^0 \psi_{S2}^0 + f_2 \psi_{S1}^{0\,2} e^{-\kappa(r_{12}-a_2)}}{1 - f_1 f_2 e^{-2\kappa(r_{12}-a_2)}} \frac{e^{-\kappa(r_{12}-a_2)}}{r_{12}} dS \qquad [58a]$$

and

$$V_{\mathrm{el}}^2 = \frac{\epsilon}{2\beta_{22}(1 + e^{-\kappa L})} \int_{S_2} \left[\frac{\psi_{S1}^0 \psi_{S2}^0 + f_1 \psi_{S2}^{0\,2} e^{-\kappa r_{21}}}{1 - f_1 f_2 e^{-2\kappa r_{21}}} e^{-\kappa r_{21}} + \frac{\psi_{S1}^0 \psi_{S2}^0 + f_1 \psi_{S2}^{0\,2} e^{-\kappa(L-r_{21})}}{1 - f_1 f_2 e^{-2\kappa(L-r_{21})}} e^{-\kappa(L-r_{21})} \right] dS. \qquad [58b]$$

Summing these expressions, and applying Eqs. [50a] and [50b], we obtain

$$V_{\mathrm{el}} = \pi \epsilon a_2 \frac{1 + e^{-\kappa(h_2-h_1)}}{1 + e^{-\kappa L}} \left\{ \frac{f_2 \psi_{S1}^{0\,2} + f_1 \psi_{S2}^{0\,2}}{f_1 f_2} \ln(1 - f_1 f_2 e^{-2\kappa h_1}) + \frac{4\psi_{S1}^0 \psi_{S2}^0}{\sqrt{|f_1 f_2|}} \begin{bmatrix} \tan^{-1}(\sqrt{|f_1 f_2|} e^{-\kappa h_1}), & f_1 f_2 < 0 \\ \tanh^{-1}(\sqrt{f_1 f_2} e^{-\kappa h_1}), & f_1 f_2 > 0 \end{bmatrix} \right\},$$

$$h_2 \geq h_1. \qquad [59]$$

4.3.4. Sphere in a Spherical Pore

Let us consider a spherical particle (entity 2) of radius a_2 in a spherical pore (entity 1) of radius a_1 shown in Fig. 5. Let h be the closest surface-to-surface distance between the particle and the pore and R be the center-to-center distance between the particle and the pore. r_{12} and r_{21} represent, respectively, the distance between the center of the particle and the surface of the pore and that between the center of the pore and the surface of the particle. Using Table 1, Eqs. [39a] and [39b] can be approximated, respectively, by

$$V_{\mathrm{el}}^1 = \frac{\epsilon a_2}{2\beta_{11}} \int_{S_1} \frac{\psi_{S1}^0 \psi_{S2}^0 + f_2 \psi_{S1}^{0\,2} e^{-\kappa(r_{12}-a_2)}}{1 - f_1 f_2 e^{-2\kappa(r_{12}-a_2)}} \frac{e^{-\kappa(r_{12}-a_2)}}{r_{12}} dS \qquad [60a]$$

and

$$V_{\mathrm{el}}^2 = \frac{\epsilon a_1}{2\beta_{22}} \int_{S_2} \left[\frac{\psi_{S1}^0 \psi_{S2}^0 + f_1 \psi_{S2}^{0\,2} e^{-\kappa(r_{21}-a_1)}}{1 - f_1 f_2 e^{-2\kappa(r_{21}-a_1)}} \frac{e^{-\kappa(r_{21}-a_1)}}{r_{21}} \right] dS. \qquad [60b]$$

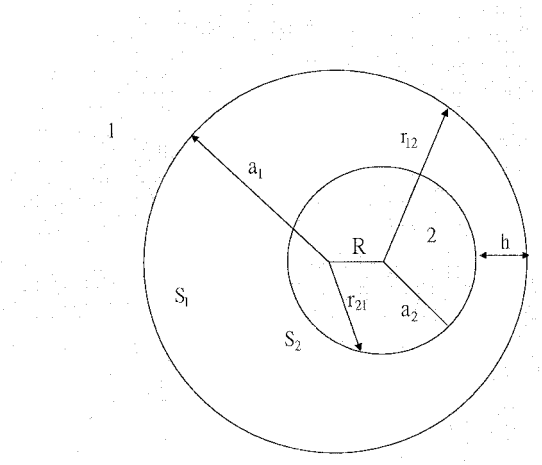

FIG. 5. A spherical particle (entity 2) of radius a_2 and a spherical pore (entity 1) of radius a_1. h is the closest surface-to-surface distance between particle and pore, R is the center-to-center distance between particle and pore, r_{12} and r_{21} denote the distance from the center of the particle to the surface of the pore and that from the center of the pore to the surface of the particle, respectively.

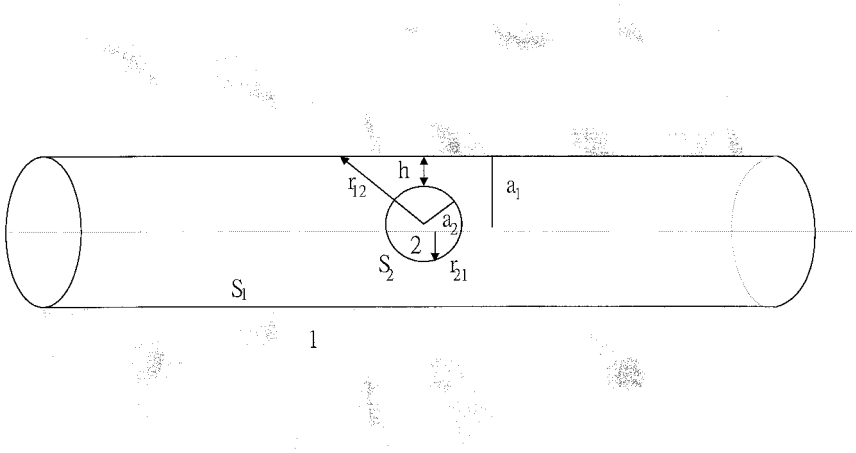

FIG. 6. A spherical particle (entity 2) of radius a_2 in a cylindrical pore (entity 1) of radius a_1. h is the closest surface-to-surface distance between particle and pore, and r_{12} and r_{21} the distance measured from the center of the particle to the surface of the pore and that from the axis of the pore to the surface of the particle, respectively.

For thin double layers, applying Eqs. [50a] and [50b] gives

$$V_{el} = \pi\epsilon a_1 a_2 \frac{1 - e^{-2\kappa R}}{R} \left\{ \frac{f_2\psi_{S1}^{0\,2} + f_1\psi_{S2}^{0\,2}}{f_1 f_2} \ln(1 - f_1 f_2 e^{-2\kappa h_1}) + \frac{4\psi_{S1}^0\psi_{S2}^0}{\sqrt{|f_1 f_2|}} \begin{bmatrix} \tan^{-1}(\sqrt{|f_1 f_2|}e^{-\kappa h_1}), & f_1 f_2 < 0 \\ \tanh^{-1}(\sqrt{f_1 f_2}e^{-\kappa h_1}), & f_1 f_2 > 0 \end{bmatrix} \right\}. \quad [61]$$

If the centers of the particle and the pore coincide, $R = 0$, and V_{DL} can be derived from Eqs. [38a] and [38b]. We have

$$V_{el} = \frac{2\pi\epsilon}{(1 - f_1 f_2 \theta_{12}\theta_{21})} \left\{ a_1^2\theta_{12} \frac{\psi_{S1}^0\psi_{S2}^0 + f_2\psi_{S1}^{0\,2}\theta_{21}}{\beta_{11}} + a_2^2\theta_{21} \frac{\psi_{S1}^0\psi_{S2}^0 + f_1\psi_{S2}^{0\,2}\theta_{12}}{\beta_{22}} \right\}. \quad [62]$$

4.3.5. Sphere Inside/Outside a Cylindrical Pore

Let us consider a spherical particle (entity 2) of radius a_2 in a cylindrical pore (entity 1) of radius a_1 illustrated in Fig. 6. Here, h is the closest surface-to-surface distance between the particle and the pore, and r_{12} and r_{21} are, respectively, the distance between the center of the particle and the surface of the pore and that between the axis of the pore and the surface of the particle. Using Table 1, Eqs. [39a] and [39b] can be approximated, respectively, by

$$V_{el}^1 = \frac{\epsilon a_2}{2\beta_{11}} \int_{S_1} \frac{\psi_{S1}^0\psi_{S2}^0 + f_2\psi_{S1}^{0\,2}e^{-\kappa(r_{12}-a_2)}}{1 - f_1 f_2 e^{-2\kappa(r_{12}-a_2)}} \frac{e^{-\kappa(r_{12}-a_2)}}{r_{12}} dS_1 \quad [63a]$$

and

$$V_{el}^2 = \frac{\epsilon a_1}{2\beta_{22}} \int_{S_2} \left[\frac{\psi_{S1}^0\psi_{S2}^0 + f_1\psi_{S2}^{0\,2}\dfrac{I_0(\kappa r_{21})}{I_0(\kappa a_1)}}{1 - f_1 f_2 \left(\dfrac{I_0(\kappa r_{21})}{I_0(\kappa a_1)}\right)^2} \frac{I_0(\kappa r_{21})}{I_0(\kappa a_1)} \right] dS_2. \quad [63b]$$

In the derivation of Eq. [63a], θ_{21} in the bracket of the right-hand side of [39a] is approximated by $\exp[-\kappa(r_{12} - a_2)]$. Although obtaining an analytical expression for V_{el}^1 and V_{el}^2 becomes difficult in this case, they can be estimated by integrating numerically the right-hand sides of Eqs. [63a] and [63b]. In a study of a similar problem where a sphere is placed axisymmetrically in a cylindrical pore, Pujar and Zydney (70) were able to derive an analytical expression for electrical potential and an approximate expression for electrical interaction energy. The former is based on a method proposed by Smith and Deen (71) and involves a harmonic expansion, the coefficients of which needed to be determined through a complicated procedure. The performance of the present boundary integral method and that of Pujar and Zydney (70) are found to be comparable (42). Note that the derivation of Eqs. [63a] and [63b] does not require axisymmetry.

If the sphere is outside the cylindrical pore, Eqs. [63] and [63b] are still applicable except that the r_{12} in the former is now defined as the distance between the center of the sphere and the surface of the cylindrical pore, and r_{21} and I_0 in the latter are replace by the distance between the axis of the pore and the surface of the sphere, and K_0, the modified Bessel function of the first kind of zero order, respectively.

5. MORE COMPLICATED PROBLEMS

The systematic approach introduced in Section 4 can also be applied to various more complicated problems of practical significance. Several examples are illustrated.

5.1. Spheres with a Membrane Layer

Let us consider two spherical particles; each comprises a rigid core and a membrane phase, which contains fixed charges of density ρ_i. In this case, Eqs. [24] and [25] must be modified, respectively, as (72)

$$\psi = \sum_{i=1}^{2} \left\{ \int_{S_i} \left[\frac{G}{\epsilon} \sigma_i + \psi_{Si} \chi_i \right] dS + \frac{1}{\epsilon} \int_{V_i} \rho_i G dV \right\} \quad [64]$$

and

$$\frac{1}{2} \psi_{Sj} = \sum_{i=1}^{2} \left\{ \int_{S_i} \left[\frac{G}{\epsilon} \sigma_i + \psi_{Si} \chi_i \right] dS_i + \frac{1}{\epsilon} \int_{V_i} \rho_i G dV \right\}. \quad [65]$$

In these expressions ψ_{Si} and σ_i are, respectively, the surface potential and surface charge density of the rigid core of particle i. If the net charge on the rigid core–membrane interface is zero, σ_i vanishes. Otherwise, the conditions regarding the interface and the membrane phase must be specified. If the distribution of fixed charge in the membrane phase is uniform, then ρ_i is constant, and Eqs. [64] and [65] can be solved. If this is not the case, then solving these equations may become difficult. For instance, ρ_i can be a function of electrical potential, which occurs if the degree of dissociation of the functional groups in the membrane phase depends upon electrical potential.

5.2. Multiple Charged Entities

The classic DLVO theory is based on the interaction between two rigid, charged particles, i.e., the concentration of particles is sufficiently low so that the probability of finding three or more particles simultaneously in a small region is negligible. If the concentration of particles is appreciable, either a statistical mechanics approach (73) or a numerical method (74) needs to be employed. Note that information about the interaction between two particles is still required in the former. Hsu and Tseng (60) proposed an iterative procedure for the resolution of Eq. [7] for multiple charged, rigid spheres under a general surface condition. The procedure has the merit that a system containing a large number of particles can be simulated by one which has relatively few particles.

Let us consider using the boundary integral method introduced in Section 4. For the case of N spheres, Eq. [24] needs to be modified as (75)

$$\psi = \sum_{i=1}^{N} \int_{S_i} \left[\frac{G}{\epsilon} \sigma_i + \psi_{Si} \chi_i \right] dS, \quad [66]$$

where

$$\chi_i = \frac{\partial G}{\partial n_i}, \; i = 1, 2, \ldots, N \quad [66a]$$

$$\frac{1}{2} \psi_{Sj} = \sum_{i=1}^{N} \int_{S_i} \left[\frac{G}{\epsilon} \sigma_i + \psi_{Si} \chi_i \right] dS_i. \quad [66b]$$

Also, Eqs. [33a], [33b], and [33e] must be modified, respectively, as

$$\Delta \underline{\psi} = [\Delta\psi_{1,1}, \ldots \Delta\psi_{1,M}, \Delta\psi_{2,1}, \ldots, \Delta\psi_{2,M}, \Delta\psi_{3,1}, \ldots, \Delta\psi_{N,M}]^t \quad [67a]$$

$$\underline{\aleph} = \begin{bmatrix} \underline{\aleph}_{1,1} & \cdot & \cdot & \cdot & \underline{\aleph}_{1,N} \\ \cdot & & & & \cdot \\ \cdot & & & & \cdot \\ \cdot & & & & \cdot \\ \underline{\aleph}_{N,1} & \cdot & \cdot & \cdot & \underline{\aleph}_{N,N} \end{bmatrix} \quad [67b]$$

and

$$\underline{B} = \begin{bmatrix} \sum_{i=2}^{N} \psi_{Si}^0 \theta_{1i,1} \\ \cdot \\ \cdot \\ \sum_{i=2}^{N} \psi_{Si}^0 \theta_{1i,M} \\ \sum_{\substack{i=1 \\ i\neq 2}}^{N} \psi_{Si}^0 \theta_{2i,1} \\ \cdot \\ \cdot \\ \sum_{\substack{i=1 \\ i\neq 2}}^{N} \psi_{Si}^0 \theta_{2i,M} \\ \cdot \\ \cdot \\ \cdot \\ \sum_{i=1}^{N-1} \psi_{Si}^0 \theta_{2i,M} \end{bmatrix}, \quad [67c]$$

where $l, k = 1, \ldots, N$. Equations [36a] and [36b] become

$$\left(\frac{1}{2} - \gamma_{ii} + \frac{\Gamma_1}{\epsilon}\beta_{ii}\right)\Delta\psi_{Si} + \sum_{\substack{i=1\\ j\neq i}}^{N}\left(\frac{\Gamma_j}{\epsilon}\beta_{ij} - \gamma_{ij}\right)\Delta\psi_{Sj} = \sum_{\substack{j=1\\ j\neq i}}^{N}\psi_{Sj}^0\theta_{ij},\ i = 1, \ldots, N. \quad [68]$$

Note that each $\Delta\psi_{Si}$ in this expression is a function. Solving this equation for $\Delta\psi_{Si}$ and substituting the resultant expression into Eq. [17] the electrical interaction energy can be determined. The results for some special cases can be found in Hsu and Liu (75).

5.3. Arbitrary-Shaped Surfaces

Since charged entities can assume various shapes in practice, a systematic approach, which is readily applicable to surfaces of an arbitrary geometry, is desirable. Hsu and Liu (76) showed that this is possible for ion-penetrable or porous particles. For rigid surfaces, the boundary integral method introduced in Section 4 is applicable if β_{ii}, β_{ji}, γ_{ii}, and γ_{ji} can be determined. However, the results based on Eqs. [29] and [37b] may not be as accurate as those for a simple geometry. In this case, Eq. [37b] needs to be derived, and Eqs. [38a] and [38b] become, respectively,

$$V_{el}^1 = \frac{\Xi_1}{2}\int_{S_1} \times \frac{\psi_2^0\left(\frac{1}{2} - \gamma_{22} + \frac{\Gamma_2}{\epsilon}\beta_{22}\right) + \psi_1\left(\gamma_{12} - \frac{\Gamma_2}{\epsilon}\beta_{12}\right)}{\left(\frac{1}{2} - \gamma_{11} + \frac{\Gamma_1}{\epsilon}\beta_{11}\right)\left(\frac{1}{2} - \gamma_{22} + \frac{\Gamma_2}{\epsilon}\beta_{22}\right) - \left(\gamma_{21} - \frac{\Gamma_1}{\epsilon}\beta_{21}\right)\left(\gamma_{12} - \frac{\Gamma_2}{\epsilon}\beta_{12}\right)} dS \quad [69a]$$

and

$$V_{el}^2 = \frac{\Xi_2}{2}\int_{S_2} \times \frac{\psi_1^0\left(\frac{1}{2} - \gamma_{11} + \frac{\Gamma_1}{\epsilon}\beta_{11}\right) + \psi_2^0\left(\gamma_{21} - \frac{\Gamma_1}{\epsilon}\beta_{21}\right)}{\left(\frac{1}{2} - \gamma_{11} + \frac{\Gamma_1}{\epsilon}\beta_{11}\right)\left(\frac{1}{2} - \gamma_{22} + \frac{\Gamma_2}{\epsilon}\beta_{22}\right) - \left(\gamma_{21} - \frac{\Gamma_1}{\epsilon}\beta_{21}\right)\left(\gamma_{12} - \frac{\Gamma_2}{\epsilon}\beta_{12}\right)} dS, \quad [69b]$$

where ψ_i^0 is the electrical potential of isolated particle i on the surface of particle j, $i \neq j$. Nevertheless, it is expected that Eqs. [29] and [37b] still provide reasonably accurate estimates for ψ_{Si}^0 and γ_{ji}, respectively. The rationale behind this is similar to that in the derivation of Eqs. [36a] and [36b] from Eqs. [31a] and [31b]. For an isolated particle j, Eqs. [24] and [25] become, respectively,

$$\psi_j = \int_{S_j}\left[\frac{G}{\epsilon}\sigma_j + \psi_{Sj}\chi_j\right]dS_j \quad [70]$$

and

$$\frac{1}{2}\psi_{Sj} = \int_{S_j}\left[\frac{G}{\epsilon}\sigma_j + \psi_{Sj}\chi_j\right]dS_j. \quad [71]$$

Since both G and χ_i become very large if a singular point is approached, as an approximation, σ_j (or ψ_{Sj}) on the right-hand sides of Eqs. [70] and [71] can be moved out from the integral sign, even if σ_j (or ψ_{Sj}) is position-dependent.

5.4. Nonequilibrium Systems

If the surface condition of an entity varies as a response to the variation in the nearby environment, the nonequilibrium behavior of the double layer near the entity should be considered. Charge-regulated surface is one of the typical examples in which the time-dependent nature of the degree of dissociation of the functional group it bears can be significant. The nonequilibrium behavior of a double layer can also be important if the distance between two charged entities varies with time. Overbeek (77), for instance, pointed out that the relaxation time for surface charges is on the order of 10^{-6} to 10^{-4} s, and the time scale for Brownian coagulation is on the order of 10^{-7} to 10^{-5} s. This implies that the contact between two particles may occur before the electrical condition reaches equilibrium. The effect of the dynamic behavior of the double layer is found to be significant also on various types of entity–entity interactions (78–86). At the present stage, methods available for the resolution of problems involving nonequilibrium electrical interactions between two charged entities are mainly numerical, and developing a systematic approach deserves further study. If the surface conditions of two entities are functions of time, but the time scale for double-layer relaxation is short, then the systematic approach introduced in Section 4 is applicable.

5.5. Primitive Models

The classic DLVO theory provides a successful theoretic prediction for the coagulation behavior of a colloidal dispersion, in particular, the Schulze–Hardy rule, which summarizes the experimental observation of the valence dependence of the critical coagulation concentration of counterions. This theory is based on the model of the electrical double layer originating

from the Göuy–Chapman theory (87, 88), in which the equilibrium electrical potential is described by Eq. [5]. Here, ions are considered as point charges and the solvent phase a continuum. Equation [5] can be viewed as a mean field approximation for the model used in the Göuy–Chapman theory where the correlation between ions is neglected, and ions are different only in their charge. Another basic assumption of the DLVO theory is that the concentration of dispersed particles is low so that the effect of the nearby particles on the interaction of two particles can be neglected. Also, their contribution to the ionic strength is negligible. The basic assumptions of the DLVO theory limit its application in the description of several important phenomena. For instance, experimental observation reveals that the critical coagulation concentration of a counterion may vary not only with the valence but also with the size of both the counterion and the coion. In the modeling of the behaviors of liquid–glass transition, polyelectrolyte suspension used in sensor, and solution containing conducting liquid crystalline polymers, the concentration of a dispersed phase is usually high and considers the interaction between two entities only becomes unrealistic. Another example is the electrical double layer near a metal–oxide surface in an aqueous electrolyte solution where water molecules play an important role in the inner Stern layer.

In the past two decades, a steady progress based on statistical mechanics in the elaboration of the effect of finite sizes of electrolyte ions on the behaviors of a dispersed phase taking the effect of their concentrations into account is observed. The so-called primitive model is capable of predicting several interesting phenomena. For example, the oscillations in spatial variations of both electrical potential and interaction force, and the electrical force between two identical charged surfaces can be attractive (30, 89–96). The effect of the sizes of the electrolyte ions on the behavior of an electrical double layer is found to be significant (97, 98). If the sizes of electrolyte ions are significant, a many-body problem needs to be considered. Often, either a statistical mechanics approach or a Monte Carlo simulation is adopted. The former involves solving the integral equations governing the spatial variation of ion–ion, particle–ion, and particle–particle correlation functions, and developing a numerical scheme is usually necessary. The statistical mechanics approach is more rigorous than the classic DLVO treatment in the sense that the finite sizes of ions and the concentration of colloidal particles are taken into account. The formulation of a problem, however, is usually complicated and a closure for correlation function needs to be assumed. Often, Coulomb's law is used to evaluate the interaction force between two charged entities, and spherical geometry is assumed for simplicity. Using this law also requires that the type of boundary conditions assumed need to be simple. These limitations can be unrealistic for cases such as polyelectrolytes and colloids with appreciable sizes. In these cases, the boundary integral method introduced in Section 4 is applicable if the free Green function is selected adequately.

6. CONCLUDING REMARKS

Evaluation of the electrical interaction energy between two charged entities in an electrolyte solution is essential to the prediction of many significant phenomena in colloid and interface science. For low electrical potentials, boundary integral method has the potential to arrive at an approximate analytical expression for electrical interaction energy under a general surface condition. Also, it is applicable to various types of surfaces and the number of charged entities. Modification of the classic double-layer model to take the finite sizes of electrolyte ions into account becomes necessary for various problems which are of both fundamental and practical significance. Developing a systematic approach for the estimation of the interaction energy is challenging in these cases. Revisiting many of the classic problems, for example, coagulation between particles, adsorption of particles to surfaces, and electrophoresis, to name a few, based on a primitive model for double layer may lead to unexpected results. Prediction and/or elaboration of the behaviors of biocolloids such as cells and microorganisms also deserve detailed study.

APPENDIX A

The electrical fore between two charged particles can be calculated by (28)

$$F = \int_{\Gamma} \left[\left(\Delta\pi + \frac{\epsilon E^2}{2} \right) \mathbf{n} - \epsilon (\mathbf{E} \cdot \mathbf{n}) \mathbf{E} \right] d\Gamma, \qquad [A1]$$

where Γ represents an arbitrary plane between two particles, $\mathbf{n}$ is the unit outer normal, and $\mathbf{E}$ the electrical field vector with strength E. The osmotic pressure, $\Delta\pi$, can be evaluated by

$$\Delta\pi = RT \sum_i n_{i\infty} \left(\exp\left(-\frac{Z_i F \psi}{RT} \right) - 1 \right). \qquad [A2]$$

For symmetric $Z{:}Z$ electrolytes Eq. [A2] becomes

$$\Delta\pi = \epsilon \left(\frac{RT}{ZF} \right)^2 \kappa^2 [\cosh(y) - 1]. \qquad [A3]$$

If the electrical potential is low, Eq. [A2] reduces to

$$\Delta\pi = \frac{\epsilon}{2} \kappa^2 \psi^2. \qquad [A4]$$

The electrical interaction energy, V_{el}, between two particles can be evaluated by

$$V_{el} = \int_h^\infty F(h)dh, \qquad [A5]$$

where h is the shortest surface-to-surface distance between two particles.

ACKNOWLEDGMENT

The National Science Council of the Republic of China partially financially supports this work.

REFERENCES

1. Verwey, E. J. W., and Overbeek, J. Th. G., *in* "Theory of the Stability of Lyophobic Colloids." Elsevier, Amsterdam, 1948.
2. Martinez, M. A., *Solid State Technol.* **37,** 26 (1994).
3. Patrick, W. J., Guthrie, W. L., Standley, C. L., and Schiable, P. M., *J. Electrochem. Soc.* **138,** 1778 (1991).
4. Israelachvili, J. N., and Adams, G., *J. Chem. Soc., Faraday Trans. 1* **74,** 975 (1978).
5. Ducker, W. A., Senden, T. J., and Pashley, R. M., *Nature* **353,** 239 (1991).
6. Hunter, R. J., *in* "Foundations of Colloid Science," Vol. 1. Oxford University Press, London, 1989.
7. Hsu, J. P., and Liu, B. T., *J. Colloid Interface Sci.* **192,** 481 (1997).
8. Hsu, J. P., Kuo, Y. C., and Chang, Y. I., *Colloid Polym. Sci.* **272,** 946 (1994).
9. Ninham, B. W., and Parsegian, V. A., *J. Theor. Biol.* **31,** 405 (1971).
10. Chan, D., Perram, J. W., White, L. R., and Healy, T. W., *J. Chem. Soc., Faraday Trans. 1* **71,** 1046 (1975).
11. Chan, D., Healy, T. W., and White, L. R., *J. Chem. Soc., Faraday Trans. 1* **72,** 2844 (1976).
12. Prieve, D. C., and Ruckenstein, E., *J. Theor. Biol.* **56,** 205 (1976).
13. Prieve, D. C., and Ruckenstein, E., *J. Colloid Interface Sci.* **63,** 317 (1978).
14. Healy, T. W., Chan, D., and White, L. R., *Pure Appl. Chem.* **52,** 1207 (1980).
15. Chang, Y. I., and Hsu, J. P., *J. Theor. Biol.* **147,** 509 (1990).
16. Hsu, J. P., Hsu, W. C., and Chang, Y. I., *J. Colloid Interface Sci.* **165,** 1 (1994).
17. Hsu, J. P., and Kuo, Y. C., *Langmuir* **13,** 4372 (1997).
18. Ettelaie, R., and Buscall, R., *Adv. Colloid Interface Sci.* **61,** 131 (1995).
19. Seaman, G. V., *in* "The Red Blood Cells" (D. M. Sergenor, Ed.), Vol. 2, p. 1136. Academic Press, New York, 1975.
20. Wunderlich, R. W., *J. Colloid Interface Sci.* **88,** 385 (1982).
21. Levine, S., Levine, M., Sharp, K. A., and Brooks, D. E., *Biophys. J.* **42,** 127 (1983).
22. Sharp, K. A., and Brooks, D. E., *Biophys. J.* **47,** 563 (1985).
23. Reiss, H., and Bassignana, I. C., *J. Membrane Sci.* **11,** 219 (1982).
24. Selvey, C., and Reiss, H., *J. Membrane Sci.* **23,** 11 (1985).
25. Ohshima, H., and Kondo, T., *J. Colloid Interface Sci.* **155,** 499 (1993).
26. Hsu, J. P., Lin, D. P., and Tseng, S. J., *Colloid Polymer Sci.* **273,** 271 (1995).
27. Carnie, S. L., and Chan, D. Y. C., *J. Colloid Interface Sci.* **161,** 260 (1993).
28. Bell, G. M., Levine, S., and McCartney, L. N., *J. Colloid Interface Sci.* **33,** 335 (1970).
29. McCormack, D., Carnie, S. L., and Chan, D. Y. C., *J. Colloid Interface Sci.* **169,** 177 (1995).
30. Medina-Noyola, M., and McQuarrie, D. A., *J. Chem. Phys.* **73,** 6279 (1980).
31. Waisman, E., and Lebowitz, J. L., *J. Chem. Phys.* **56,** 3086 (1972).
32. Belloni, N., *J. Chem. Phys.* **88,** 5143 (1988).
33. Krieger, I. M., and Hiltner, P. A., *in* "Polymer Colloids" (R. M. Fitch, Ed.), p. 63. Plenum Press, New York, 1971.
34. Kirkwood, J. G., and Mazur, J., *J. Polym. Sci.* **9,** 519 (1952).
35. Kaldasch, J., Laven, J., and Stein, H. N., *Langmuir* **12,** 6197 (1996).
36. Derjaguin, B. V., and Landau, L. D., *Acta Phys.-Chim. USSR* **14,** 633 (1941).
37. Wang, H. P., Jin, J., and Blum, L., *Colloid Polym. Sci.* **273,** 359 (1995).
38. Wang, H. P., Jin, J., and Blum, L., *Colloid Polym. Sci.* **273,** 947 (1995).
39. Belouschek, P., Lorenz, D., and Adamczyk, Z., *Colloid Polym. Sci.* **269,** 528 (1991).
40. Ohshima, H., Healy, T. W., and White, L. R., *J. Colloid Interface Sci.* **89,** 484 (1982).
41. Ohshima, H., Chan, D. Y. C., Healy, T. W., and White, L. R., *J. Colloid Interface Sci.* **92,** 232 (1983).
42. Hsu, J. P., and Liu, B. T., *J. Chem. Phys.* **110,** 25 (1999).
43. Stankovich, J., and Carnie, S. L., *Langmuir* **12,** 1453 (1996).
44. Anandarajah, A., and Chen, J., *J. Colloid Interface Sci.* **168,** 111 (1994).
45. Carnie, S. L., Chan, D. Y. C., and Stankovich, J., *J. Colloid Interface Sci.* **165,** 116 (1994).
46. Chan, B. K. C., and Chan, D. Y. C., *J. Colloid Interface Sci.* **92,** 281 (1983).
47. James, A. E., and Williams, D. J. A., *J. Colloid Interface Sci.* **107,** 44 (1985).
48. You, Y. J., and Harvey, C., *J. Comput. Chem.* **14,** 484 (1993).
49. Chou Chang, F. R., and Sposito, G., *J. Colloid Interface Sci.* **163,** 19 (1994).
50. Bowen, W. R., and Sharif, A. O., *J. Colloid Interface Sci.* **187,** 363 (1997).
51. Deryaguin, B. V., *Kolloid Z.* **69,** 155 (1934).
52. Hogg, R., Healy, T. W., and Fuerstenau, D. W., *Trans. Faraday Soc.* **62,** 1638 (1966).
53. Sader, J. E., Carnie, S. L., and Chan, D. Y. C., *J. Colloid Interface Sci.* **171,** 46 (1995).
54. Wang, H. P., and Jin, J., *J. Colloid Interface Sci.* **177,** 380 (1996).
55. Bhattacharjee, S., and Elimelech, M., *J. Colloid Interface Sci.* **193,** 273 (1997).
56. Krozel, J. W., and Saville, D. A., *J. Colloid Interface Sci.* **150,** 365 (1992).
57. Kijlstra, J., *J. Colloid Interface Sci.* **153,** 30 (1992).
58. Carnie, S. L., Chan, D. Y. C., and Gunning, J. S., *Langmuir* **10,** 2993 (1994).
59. Glendinning, A. B., and Russel, W. B., *J. Colloid Interface Sci.* **93,** 95 (1983).
60. Hsu, J. P., and Tseng, M. T., *J. Chem. Phys.* **104,** 242 (1996).
61. Ohshima, H., *J. Colloid Interface Sci.* **162,** 487 (1994).
62. Ohshima, H., *Colloid Polym. Sci.* **274,** 1176 (1996).
63. Ohshima, H., *J. Colloid Interface Sci.* **198,** 42 (1998).
64. Tsao, H. K., *J. Colloid Interface Sci.* **205,** 538 (1998).
65. Hsu, J. P., and Liu, B. T., *J. Colloid Interface Sci.* **190,** 371 (1997).
66. Ohshima, H., *J. Colloid Interface Sci.* **176,** 7 (1995).
67. Greenberg, M. D., *in* "Application of Green's Functions in Science and Engineering." Prentice-Hall, Englewood Cliffs, NJ, 1971.
68. Jeffreys, H., and Jeffreys, B. S., *in* "Methods of Mathematical Physics." Cambridge University Press, Cambridge, 1956.
69. McCartney, L. N., and Levine, S., *J. Colloid Interface Sci.* **30,** 345 (1969).
70. Pujar, N. S., and Zydney, A. L., *J. Colloid Interface Sci.* **192,** 338 (1997).
71. Smith, F. G., and Deen, W. M., *J. Colloid Interface Sci.* **78,** 444 (1980).
72. Hsu, J. P., and Liu, B. T., *Chem. Phys.* **236,** 63 (1998).
73. Hsu, J. P., and Liu, B. T., *J. Phys. Chem. B* **102,** 334 (1998).
74. Reiner, E. S., and Radke, C. J., *AIChE. J.* **37,** 805 (1991).
75. Hsu, J. P., and Liu, B. T., *J. Phys. Chem. B* **102,** 8492 (1998).
76. Hsu, J. P., and Liu, B. T., *J. Phys. Chem. B* **102,** 3892 (1998).
77. Overbeek, J. Th. G., *J. Colloid Interface Sci.* **58,** 408 (1977).
78. Kijlstra, J., and van Leeuwen, H. P., *J. Colloid Interface Sci.* **160,** 424 (1993).

79. Lyklema, J., *Pure Appl. Chem.* **52,** 1221 (1980).
80. Lyklema, J., *in* "The Structure, Dynamics and Equilibrium Properties of Colloidal Systems" (D. M. Bloor and E. Wyn-Jones, Eds.), Kluwer Academic, Dordrecht, 1990.
81. Dukhin, S. S., and Lyklema, J., *Langmuir* **3,** 94 (1987).
82. Hsu, J. P., and Kuo, Y. C., *J. Chem. Soc. Faraday Trans.* **91,** 4093 (1995).
83. Shulepov, S. Yu, Dukhin, S. S., and Lyklema, J., *J. Colloid Interface Sci.* **171,** 340 (1995).
84. Mandralis, Z., Wernet, J. H., and Feke, D. L., *J. Colloid Interface Sci.* **182,** 26 (1996).
85. Krozel, J. W., *J. Colloid Interface Sci.* **163,** 437 (1994).
86. Hsu, J. P., Kuo, Y. C., and Tseng, S. J., *J. Colloid Interface Sci.* **195,** 388 (1997).
87. Gouy, G., *J. Phys. Radium* **9,** 457 (1910).
88. Chapman, D. L., *Phil. Mag.* **25,** 475 (1913).
89. Lozada-Cassou, M., *J. Chem. Phys.* **80,** 3344 (1984).
90. Lozada-Cassou, M., and Diaz-Herrera, E., *J. Chem. Phys.* **92,** 1194 (1990).
91. Lozada-Cassou, M., and Diaz-Herrera, E., *J. Chem. Phys.* **93,** 1386 (1990).
92. Levesque, D., Weis, J. J., and Patey, G. N., *J. Chem. Phys.* **72,** 1887 (1980).
93. Patey, G. N., *J. Chem. Phys.* **72,** 5763 (1980).
94. Teubner, M., *J. Chem. Phys.* **75,** 1907 (1981).
95. Valleau, J. P., Ivkov, R., and Torrie, G. M., *J. Chem. Phys.* **95,** 520 (1991).
96. Chu, X., and Wasan, D. T., *J. Colloid Interface Sci.* **184,** 268 (1996).
97. Blum, L., *J. Chem. Phys.* **81,** 136 (1977).
98. Henderson, D., and Blum, L., *J. Chem. Phys.* **69,** 5441 (1978).